Available online at www.sciencedirect.com
SCIENCE DIRECT®
Journal of Power Sources 141 (2005) 177–187
JOURNAL OF POWER SOURCES
www.elsevier.com/locate/jpowsour

Development of gas-separation membrane-assisted lead-acid battery

A.F. Ismail*, W.A. Hafiz

Membrane Research Unit, Faculty of Chemical and Natural Resources Engineering, Universiti Teknologi Malaysia, 81310 Skudai, Johor, Malaysia

Received 28 May 2004; received in revised form 21 July 2004; accepted 27 September 2004
Available online 8 December 2004

Abstract

The objective of this study is to improve the design of a starting, lighting and ignition (SLI) lead-acid battery with the introduction of gas-separation membrane technology that functions as an electrolyte retainer. Asymmetric polysulfone gas-separation flat-sheet membranes were applied on the battery vent holes that is charged at 15 A and the electrolyte loss data were monitored and compared to the conventional battery. Effects of polymer concentration and casting shear rate were investigated in order to produce the most suitable gas-separation membrane, which features minimal electrolyte losses during the charging test. At room temperature, the electrolyte losses of a membrane-assisted lead-acid battery are about 6.67 g h^{-1}, while for a conventional battery it is about 26.67 g h^{-1}. During the charging process at a temperature of about 80 °C, the membrane-assisted lead-acid battery can save up to 40% of electrolyte losses compared to the conventional battery.

Keywords: Lead-acid battery; Electrolyte losses; Gas-separation membrane

1. Introduction

Since 1980, there has been a rapid increase in the demand and manufacturing sector for the lead-acid battery. Together with developing the motor vehicle manufacturing sector, the lead-acid battery industry has never been so competitive, with so many companies that were brought up in manufacturing lead-acid batteries. It has been proven that lead-acid batteries have played a critical role as the most reliable power source in automotive, portable and remote electrical applications all over the globe [1–5].

The lead-acid battery, especially in tropical countries, has a critical water decomposition problem that seems to be deteriorating its life cycle and performance. The combination of overcharging and hot weather contributes to high water losses in lead-acid batteries [6,7]. This causes the decrease in electrolyte. Whenever the electrolyte level goes down, the acid concentration becomes stronger and this leads to an important increase in the rate of self-discharge [8]. In addition, the consumer has to top up the electrolyte level every time it goes lower than its minimum level. These are some of the problems faced in the flooded starting, lighting and ignition (SLI) batteries that need to be reviewed in its design in order to improve the performance.

Some manufacturers introduced the so-called "maintenance-free" batteries that uses gelled-electrolyte in their products. However, it is a disappointment that this immobilized electrolyte fails to operate in hot engine condition as reported in oriental cars, where the temperature inside the booth compartment can reach up to 60–80 °C. Therefore, it is a thought that the application of a gas-separation membrane would be ideal in solving the water decomposition problem in lead-acid batteries. The membrane, which acts as a selective barrier, retains electrolyte by controlling or minimizing the rate of vaporized electrolyte disposal into the atmosphere. In gas-separation membrane-assisted lead-acid battery, the membrane would be affixed to a battery by

* Corresponding author. Tel.: +60 7 5535592; fax: +60 7 5581463.
E-mail address: afauzi@utm.my (A.F. Ismail).

0378-7753/$ – see front matter © 2004 Elsevier B.V. All rights reserved.
doi:10.1016/j.jpowsour.2004.09.028

forming a certain design size and mounted below the vent plug. The common vent plug is used to discharge pressure build-up through the membranes.

In the emergence of the so-called maintenance-free batteries produced by manufacturers, many technologies have been introduced in order to overcome the electrolyte loss problem. Among those were the approaches of the valve-regulated lead-acid (VRLA) battery [9–12], absorptive glass mat (AGM) or gelled-electrolyte-based sealed lead-acid (SLA) batteries [13–17], additional electrolyte volume [18] and the suppression of H_2 evolution and O_2 reduction effect [19,20]. Therefore, this research is considered as a revolutionary step in the establishing of a new age of maintenance-free battery with the introduction of gas-separation membrane technology into the lead-acid battery.

2. Methodology

The experiments have been divided into two parts that consist of membrane preparation and testing on a lead-acid battery during the charging process.

2.1. Membrane preparation

Polysulfone (Udel bisphenol A polysulfone (Udel P1700)) (purchased from Amoco Performance Products) was selected as the membrane material because of the commercial availability, ease of processing and favourable selectivity–permeability characteristics, mechanical and thermal properties, durability to high acidity conditions and its cost effectiveness. Polysulfone (PSF) is an amorphous glassy polymer, containing sulfone group, ether linkages and aromatic nuclei in the polymer backbone. All the chemicals used such as *N*,*N*-dimethylacetamide (DMAc), dimethylformamide (DMF) ethanol and tetrahydrofuran (THF) were analytical grade and purchased from Aldrich Co. and used as received.

The membranes applied on lead-acid batteries were prepared by casting a polymer solution consisting of 13% (w/w) of polysulfone (PSF) and 87% (w/w) of *N*-*N*-dimethylformamide (DMF). The casting process was performed by using a pneumatically controlled casting machine. The casting solution was cast on a glass plate with a casting knife gap setting of 150 μm. In this analysis, two membrane fabrication parameters were manipulated in order to get the most suitable membrane that it going to be applied on the battery, namely the polymer concentration and shear rate during the casting process.

2.2. Membrane-assisted lead-acid battery charging test

After various types of membranes were fabricated, these membranes were then tested on lead-acid batteries to find out whether they are capable of maintaining the electrolyte level inside the battery. In order to put the membrane up to the real test, the membrane is applied on the battery cap and then the battery is charged by an alternator. This analysis is done in three stages to optimize the fabricating conditions so that electrolyte losses can be minimized. The tests were done accordingly as below:

(i) First stage
- Preliminary membrane-assisted lead-acid battery charging test.

(ii) Intermediate stage
- Membrane-assisted lead-acid battery charging test.

(iii) Final stage
- Membrane-assisted lead-acid battery charging test with heat supply.

2.2.1. Preliminary membrane-assisted lead-acid battery charging test

This test is done to screen down to the suitable membrane formulation to be used in the membrane-assisted lead-acid battery charging test. There are eight different types of membrane with different formulations that were successfully cast; the solution formulations are given in Table 1. Through this preliminary test, all the membranes fabricated in the earlier stage were cut accordingly to the battery vent hole size and then applied on each of the six lead-acid battery vent holes with epoxy adhesive to prevent any leakages. Then the battery is continuously charged using an alternator and charged on average at 15 A. The objective of this test is to select a membrane formulation with the most suitable polymer concentration. This is done by observing the electrolyte level inside the battery. The membrane that has the most retained electrolyte level throughout the experiment will be the chosen one. A control test run without any application of membrane on the battery holder, was done to differentiate how much electrolyte losses can be minimized. Prior to this screening process, the selected membrane formulation will proceed to the second stage experiment, which is the membrane-assisted lead-acid battery charging test.

Table 1
Casting solution formulations

Polymer solution composition	GS1 (%)	GS2 (%)	GS3 (%)	GS4 (%)	GS5 (%)	GS6 (%)	GS7 (%)	GS8 (%)
Polysulfone (PSF)	22	18.7	15.2	20	15	13	12.5	11
N,*N*-dimethylacetamide (DMAc)	31.8	33.2	34.6	–	–	–	–	–
Dimethylformamide (DMF)	–	–	–	80	85	87	87.5	89
Tetrahydrofuran (THF)	31.8	33.2	34.6	–	–	–	–	–
Ethanol	14.4	14.9	15.6	–	–	–	–	–

2.2.2. Membrane-assisted lead-acid battery charging test

After the first stage of experiment has been established, the most suitable membrane formulation will be chosen and reproduced with different casting shear rates. The objective of this experiment is to determine the best shear rate so that the electrolyte losses can be further minimized. Therefore, during the membrane-assisted lead-acid battery charging test with heat supply, the performance is already optimized.

As the membranes were produced with different shear rates, they were cut into circular sheets with the diameter of 3.5 cm. The membrane was applied into the battery cap as shown in Fig. 1. Subsequently, this spiral end stainless steel battery cap is applied on the battery vent hole and then sealed with epoxy sealant to prevent any leakages. Charged using an alternator at the average rate of 15 A, the battery is charged for approximately three straight hours. Gas permeation from the battery cap is measured as such shown in Fig. 2, where it uses the principle of a soap bubble flow meter. During this experiment, three parameters were observed, namely the flow rate of the permeating vaporized electrolyte, the electrolyte losses and the pressure build-up measured inside battery. At the end of the experiment, the membrane with the best casting shear rate will be selected and will proceed to the final stage of the experiment. The best casting shear will be expected to exhibit the best performance in minimizing electrolyte losses as well as minimizing pressure build-up.

2.2.3. Membrane-assisted lead-acid battery charging test with heat supply

This experiment will be the third and the final stage experiment in evaluating the effectiveness of membrane application on a lead-acid battery. It is quite similar to the membrane-assisted lead-acid battery charging test, where all of the equipment configurations are all the same except that there is a water bath inclusion for this experiment. The objective of this test is to investigate the effect of heat supply to the battery on the electrolyte losses. The membrane with the most suitable polymer concentration and casting shear rate which is determined from the two previous experiments, will be tested in this experiment to observe the effectiveness of the membrane in retaining electrolyte when in a high-temperature condition.

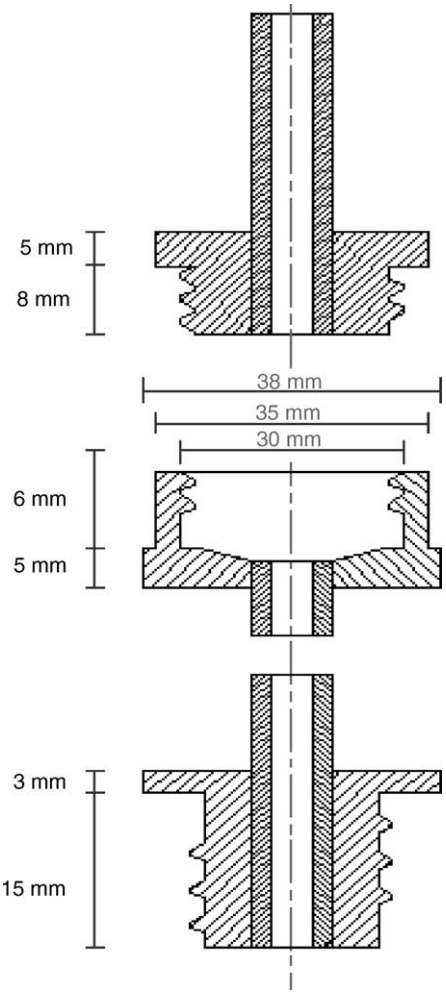

Fig. 1. Schematic drawing and cross-section of battery cap.

Similar to the membrane-assisted lead-acid battery charging test, membranes are cut into circular sheets with the diameter of 3.5 cm and applied into battery caps as shown in Fig. 1. Subsequently, this spiral end stainless steel battery

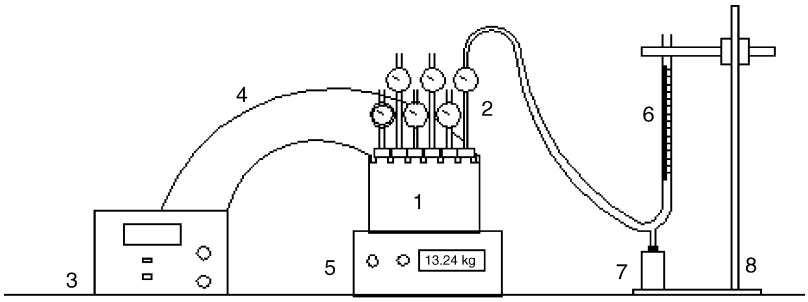

(1) Lead -Acid Battery; (2) Membrane Holder with Pressure Gauge;
(3) Alternator, (4) Electrical Wire; (5) Weight scale;
(6) Burrette; (7) Soap Solution; (8) Retort Stand.

Fig. 2. Membrane-assisted lead-acid battery charging test apparatus.

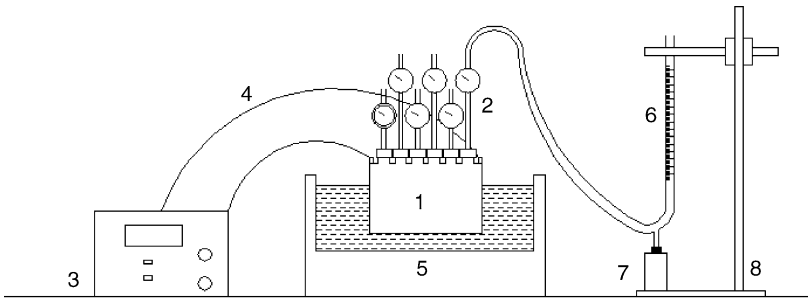

(1) Lead-Acid Battery; (2) Membrane Holder with Pressure Gauge;
(3) Alternator; (4) Electrical Wire; (5) Water Bath with Heater;
(6) Burrette; (7) Soap Solution; (8) Retort Stand.

Fig. 3. Membrane-assisted lead-acid battery charging test with heat supply apparatus.

cap is applied on the battery vent hole, and then sealed with epoxy sealant to prevent any leakages. Charged using an alternator at the average rate of 15 A, the battery is charged for approximately three straight hours. This time, instead of placing the lead-acid battery on a weight scale, it is put inside a temperature-controlled water bath, as shown in Fig. 3. To measure the water losses from the lead-acid battery, the initial mass of the battery is measured before starting the experiment. After the test is done the mass of the battery is measured again to see the electrolyte losses.

3. Results and discussion

3.1. Preliminary membrane-assisted lead-acid battery charging test result

The observation done was based on electrolyte level during recharging of a lead-acid battery. This is a way to simulate the charging condition inside a car when the alternator charges the battery. This condition is said to be the main factor that causes water decomposition. Hydrogen, oxygen and water vapor forms whenever overcharging of a lead-acid battery occurs. It was observed that, after a few hours of charging the membrane that was applied on top of the battery cap had swollen. Other observations were that the battery casing had also become swollen and the level of electrolyte was fluctuating. This is due to the pressure build-up inside the battery casing because of the membrane skin layer was too thick for the vaporized electrolyte to diffuse through. The next step taken after observing the battery casing being swollen was to stop the charging process.

As shown in Table 2, the results of the membrane-assisted battery test showed that ternary system solution (one polymer, one solvent, one non-solvent) membranes GS1–GS3 are still too tight as the pressure builds up inside the battery casing and causes the casing to swell. The application of binary system (one polymer, one solvent) solution cast membrane such as GS4 and GS5 have better results than those seen with the ternary system membranes. The pressure build-up featured in GS4 and GS5 took longer charging period to swell the battery casing and the weight losses are quite minimal compared to GS1–GS3. This is due to the thickness of the skin layer possessed by the ternary system (one polymer, one solvent and one non-solvent) solution cast membranes. This result agreed with the conclusion made by previous works [21,22].

Meanwhile, the lower polymer concentration membranes such as in GS6, GS7 and GS8 showed better permeability compared to the latter membranes. This is proved through the observation of battery electrolyte level and the compactness of the swollen battery casing. However, the GS7 displayed poor electrolyte retaining characteristics as water droplets emerge on its surface. Meanwhile the GS8 membrane had ruptured after the battery was charged for 1.5 h. This indicates that the polymer matrixes found in GS7 and GS8 are not that strong and compact, as those membranes permeate gases easily. As for GS6, with polymer concentration of 13.0% (w/w)

Table 2
Preliminary screening of membranes for a membrane-assisted lead-acid battery test

Membrane	Rate of electrolyte loss after charging (%)	Remarks
GS1	10	Battery casing severely swollen after 2 h of charging
GS2	10	Battery casing swollen severely after 2.5 h of charging
GS3	13	Battery casing severely swollen after 3 h of charging
GS4	13	Battery casing severely swollen after 3.25 h of charging
GS5	15	Battery casing swollen after 3.5 h of charging
GS6	15	Battery casing moderately swollen after 4 h of charging
GS7	20	Battery casing mildly swollen after 2 h of charging, but droplets of water emerge on the membrane surface
GS8	25	Battery casing mildly swollen after 1.5 h of charging, but the membrane sheet ruptured

polysulfone and 87% (w/w) of DMF solvent, it showed the best permeation of vaporized electrolyte and at the same time showed minimum pressure build-up inside the battery casing.

Even though the membranes tested exhibited some degree of case swelling, the phenomenon was considered negligible, as there was only minimal pressure build-up, especially in the GS6 membrane. The extreme degree of case swelling was only found in membranes with high polymer concentration (GS1–GS5) and it is confirmed that these membranes have failed in the preliminary test, and could not function well as water retaining devices. The GS6 membrane has shown a very promising result probably because the polymer solution formulation used was the most suitable in terms of membrane permeability and selectivity.

3.2. Membrane-assisted lead-acid battery charging test result

During the membrane-assisted lead-acid battery charging test, the most important parameter observed is the electrolyte losses. This is because the main objective of this research is to minimize the electrolyte losses from the lead-acid battery during the charging process. The membranes were cast into six different shear rates and substituted with the names as shown in Table 3. One of the main criteria in selecting the best shear rate for the membrane is its capability in retaining the electrolyte volume from being disposed into the atmosphere.

Fig. 4 shows the profile of electrolyte losses for three selected membrane shear rates and one control test. The electrolyte loss for the control test was continuously increasing until the end of the test. At the end of the 3 h experiment, the control test battery lost about 80 g of electrolyte, and has an average electrolyte losses rate of 26.67 g h^{-1}. For the membrane-assisted lead-acid battery, the electrolyte losses were found to be the coherent in shear rates of 7s, 11s and 12s, with the rate of losses of 20 g h^{-1}. Whereas for the shear rates of 8s, 9s, 10s, the average rate of electrolyte loss was found to be 6.67 g h^{-1}.

As shown in Table 4, the calculated percentage of electrolyte-loss minimization using the GS6 membrane cast

Table 3
GS6 membranes prepared with different shear rates

Membrane casting shear rate (s^{-1})	Substitute name
300	7s
262.5	8s
233.33	9s
210	10s
190.91	11s
175	12s

Table 4
Total and average rate of electrolyte losses during a membrane-assisted lead-acid battery charging test

Membrane used	Total electrolyte loss (g of electrolyte)	Rate of electrolyte loss (g h^{-1})
Control test	80	26.67
7s	60	20
8s	20	6.67
9s	20	6.67
10s	20	6.67
11s	60	20
12s	60	20

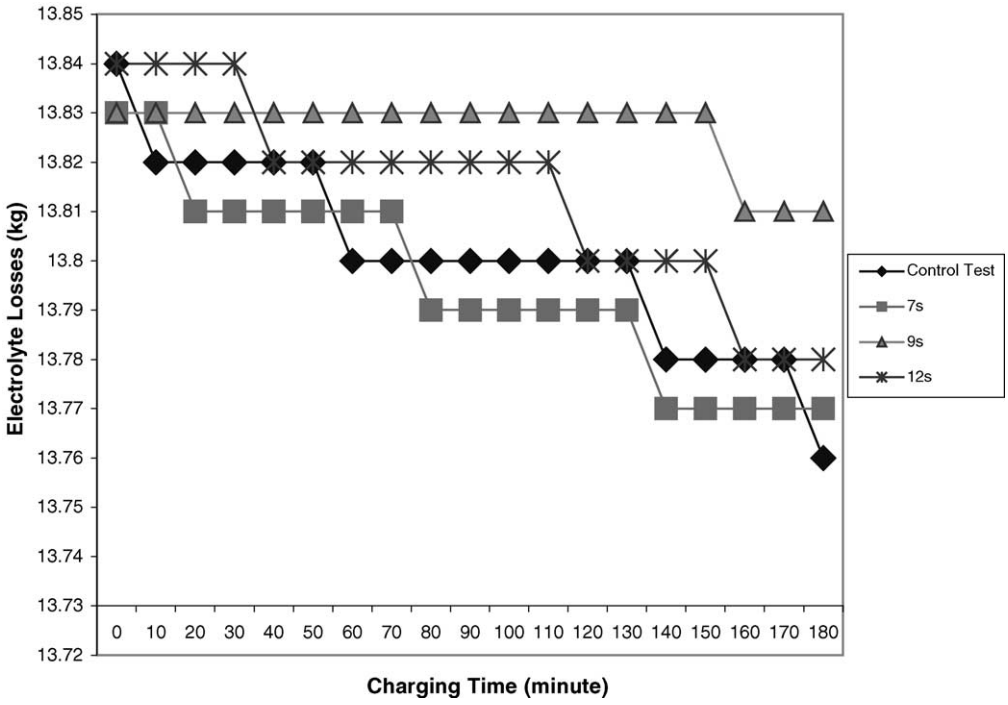

Fig. 4. Effect of shear rate on the performance of the membrane in minimizing electrolyte losses.

at different shear rates compared favourably to the conventional lead-acid battery. The percentage of electrolyte-loss minimization was calculated with the following equation:

$$\text{Percentage of electrolyte-loss (\%)} = \frac{\text{Electrolyte loss for control test} - \text{Electrolyte loss with membrane}}{\text{Electrolyte loss for control test}} \times 100 \quad (3.1)$$

Fig. 5 shows that with the application of the 7s, 11s or 12s membranes, the electrolyte losses can be minimized up to 25%. However, with the application of the 8s, 9s or 10s membranes, the electrolyte losses can be minimized with a better percentage of 75%, which is three times better than the latter. Even though it seems that the electrolyte losses in shear rates of 7s, 11s and 12s are still low, they were outshone by the performance of 8s, 9s and 10s membranes. This means that the critical shear rate must lie within the range of 210–262.5 s^{-1}.

In order to identify the critical shear rate, a comparison analysis must be made on other parameters, which are the pressure build-up inside the battery casing and the flow rate of the vaporized electrolyte profile. The critical shear rate will feature a minimal pressure build-up inside the battery casing and the smoothest flow rate profile of vaporized electrolyte.

Fig. 6 shows typical pressure profiles of pressure build-up during membrane-assisted lead-acid battery charging tests. There is no pressure profile for the control test as there was no pressure build-up since all of the vaporized electrolytes is lost through the vent hole.

Membranes cast at six different shear rates show different values of maximum pressure build-up with similar trends for the profiles. Each of the membranes had a sudden increase of pressure build-up during the first twenty minutes of charging. The next phenomenon seen after the sudden increase is the pressure build-up starts to show a tendency to become constant as the flow rate of vaporized electrolyte becomes faster.

During the first 20 min of charging, the vaporized electrolyte could not be permeated smoothly since the pressure build-up is still low. Since the membrane flux is pressure driven, the vaporized electrolyte could not permeate through the selective skin and therefore it remains trapped inside the battery casing. The pressure build-up increases until it reaches the point where the pressure becomes constant and the vaporized electrolyte permeation rate becomes constant also. This is the point when the condition reaches its "working pressure", where the pressure build-up is stabilized due to the smooth and constant permeation of vaporized electrolyte.

In selecting the critical shear rate from the six different shear rates applied, the pressure profile must feature a minimum value of "working pressure" as well as minimizing electrolyte loss during the charging process. In this case, the 9s membrane (cast at 233 s^{-1}) had the lowest pressure build-up profile with the final build-up pressure of only about 0.73 bar after three hours of charging. Compared to the other shear rates—7s membrane recorded about 0.93 bar; 8s membrane about 1.02 bar; 10s membrane about 0.88 bar; 11s membrane about 0.96 bar; 12s membrane about 0.93 bar—9s membrane has the lowest final pressure.

As shown in Fig. 7, the flow rate of gas permeation from the battery during charging in the control test is continuously increasing. This shows that electrolyte is continuously expelled without application of a membrane. Most of the membranes have shown a slow increase of vaporized electrolyte flow rate except for the 9s membrane. The rate of increase for vaporized electrolyte flow rate in the 7s, 8s,

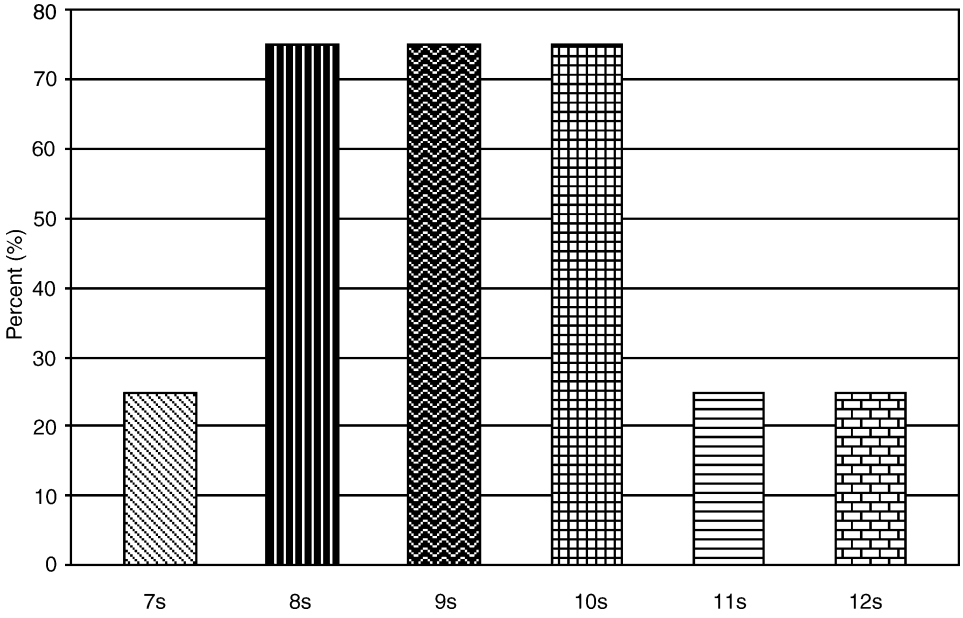

Fig. 5. Magnitude of electrolyte loss in comparison to a conventional lead-acid battery.

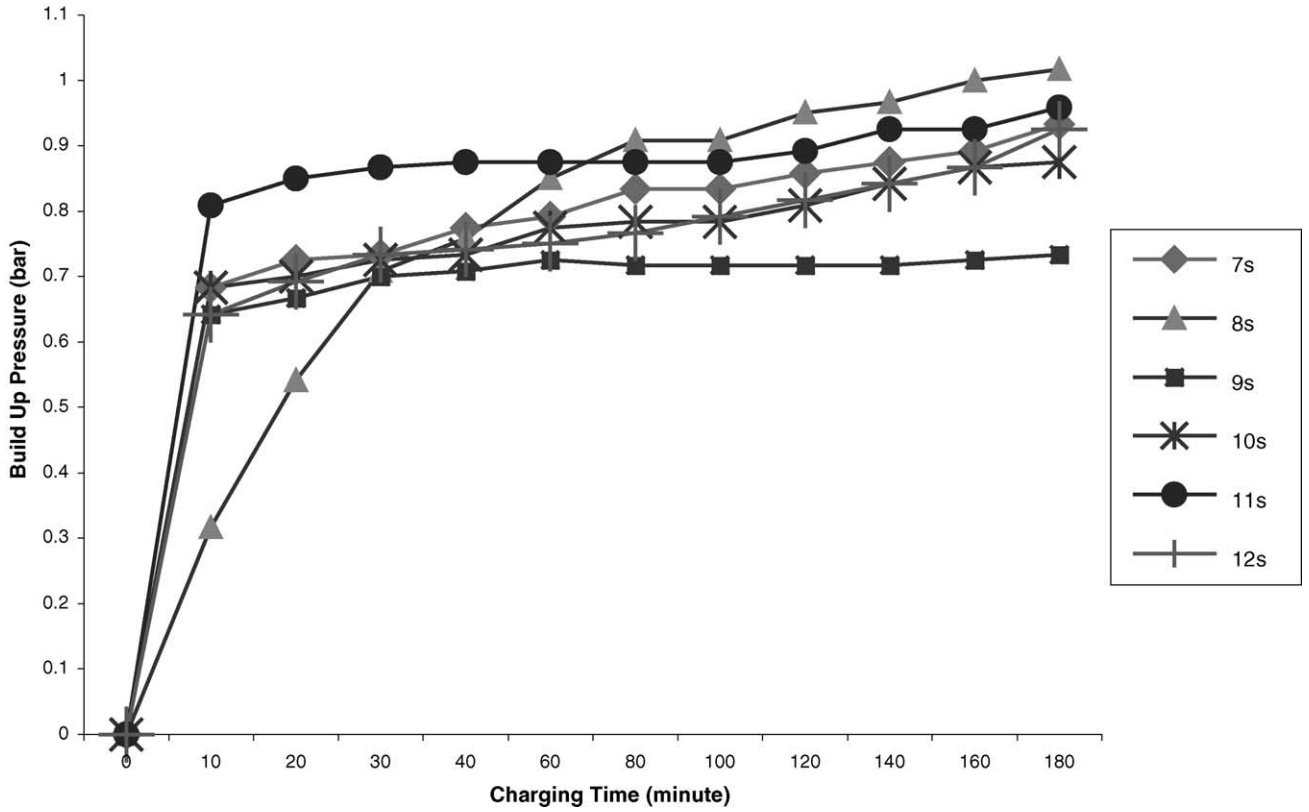

Fig. 6. Effect of shear rate on the pressure build-up inside the battery casing.

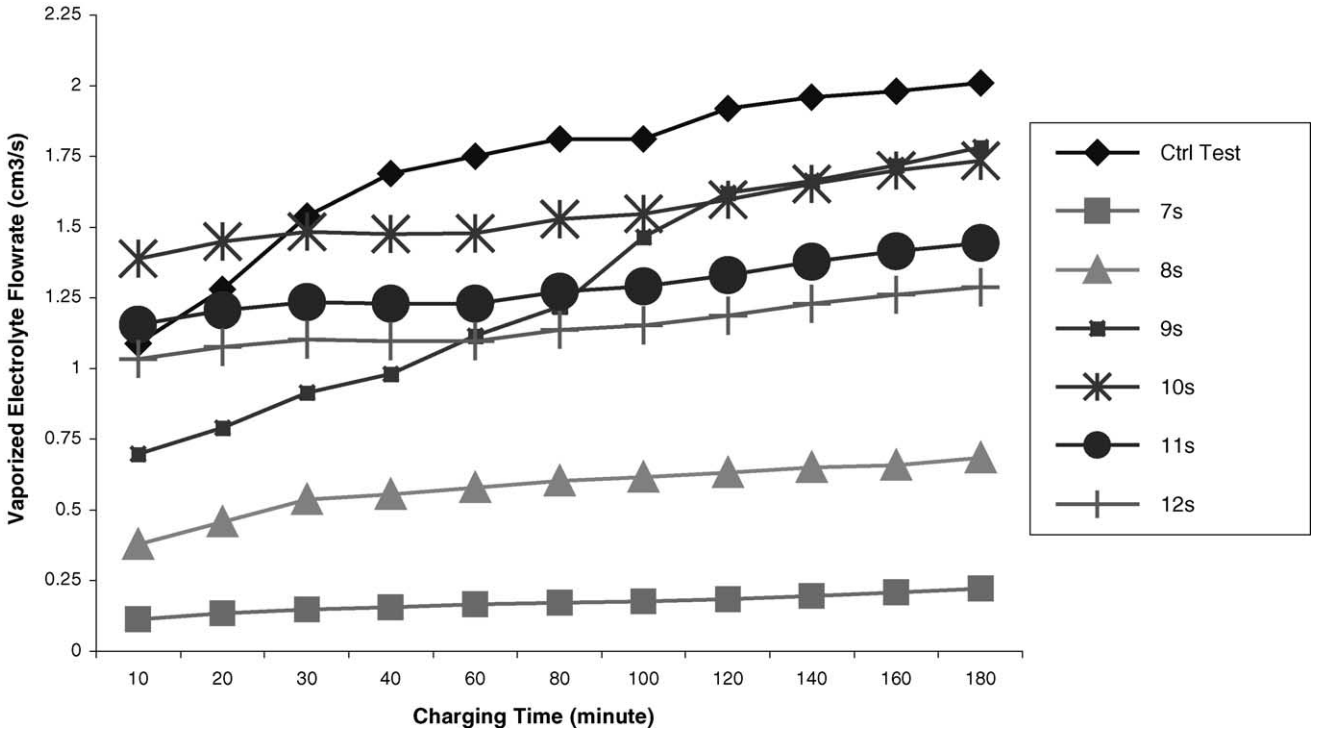

Fig. 7. Effect of shear rate on the flow rate profile of vaporized electrolyte.

10s, 11s and 12s membranes are not that distinct from what had been shown for the 9s membrane flow rate profile. The flow rate of gas permeation from the battery during charging with the application of the 9s membrane is quite slow at the early stages of charging and the rate is increasing as time elapses. During the first 60 min of charging, the 9s membrane shows a lower flow rate of vaporized electrolyte due to its electrolyte retaining characteristic. However, after the first 60 min, the 9s membranes profile almost emulates the flow rate of the control test, and this proves that the vaporized electrolyte is being well circulated inside the battery without tolerating the minimization of electrolyte losses during charging. This indicates that as charging goes along the way, the permeation of gas will continuously increase and pressure build-up inside the battery casing could be minimized.

The effect of shear experienced in the casting process on membrane properties were found to be intimately correlated to the structural knowledge at the molecular level. As shown in Figs. 6 and 7, the critical shear is selected for the performance analysis of each of the shear rates in minimizing electrolyte losses as well as in minimizing pressure build-up during the charging process. Based on the results obtained, the critical shear rate was determined to be about 233.33 s^{-1} for the 9s membrane, due to its minimal electrolyte loss and lowest pressure build-up showed among the other shear rates.

In the region prior to the critical shear rate (233.33 s^{-1}), formation of a dense skin occurs due to demixing and a precipitation mechanism, which was considered to be independent of shear rate. Increasing shear rate enhances molecular orientation in the skin layer and, in turn, improves selectivity in asymmetric membranes [23,24]. This has been demonstrated where electrolyte losses were seen to be further minimized. The permeation rate of an asymmetric membrane was also found to increase when the shear rate is approaching the critical shear. This was consistent with the reduction in skin thickness, where increasing shear rate seems to decrease skin layer thickness and the pressure build-up seems to be lowered [25].

Since the solution used in this study is shear thinning, when shear rate reached beyond the critical point (233.33 s^{-1}), a severe decrease in solution viscosity occurred, presumably due to losses in chain entanglement in solution. In this case, the membrane might undergo an instant demixing and precipitation to result in a highly oriented skin layer [26,27]. Furthermore, casting over the critical shear rate (233.33 s^{-1}), which is considered a high shear rate, could pull molecular chains or phase separated domains apart and begin to create slight defects or imperfections in the skin layer [26]. As shown in Fig. 5, casting polysulfone membranes at higher shear rates (262.15–300 s^{-1}) causes a decrease in selectivity and electrolyte losses seems to be higher than those featured near the critical shear rate region.

3.3. Membrane-assisted lead-acid battery charging test with heat supply result

As depicted in Fig. 8, the chart shows the total electrolyte losses for both batteries, membrane applied and conventional ones, during the membrane-assisted lead-acid battery charging test with the temperature set at 60 and 80 °C, respectively. This test, simulates the condition within the engine compartment, where the battery is charged at an average rate of 15 A and with the effect of high temperature of 60 and 80 °C. The objective is to observe how the membrane performs in minimizing electrolyte losses, even with the presence of an extreme temperature effect.

For the control test results, the electrolyte losses for the battery that was charged for three straight hours in a water bath set at 60 °C was 60 g. As calculated, the average electrolyte loss rate for this conventional battery is 20 g h^{-1}. Meanwhile, the electrolyte losses for the GS6-9s membrane-applied battery in the same condition was only 40 g, equivalent to an average electrolyte loss rate of 13.33 g h^{-1}. As resulted in the control test, the electrolyte loss for the battery charged for three straight hours in a water bath set at 80 °C was 100 g, while the loss for the GS6-9s membrane-applied lead-acid battery in the same condition was only 60 g. On

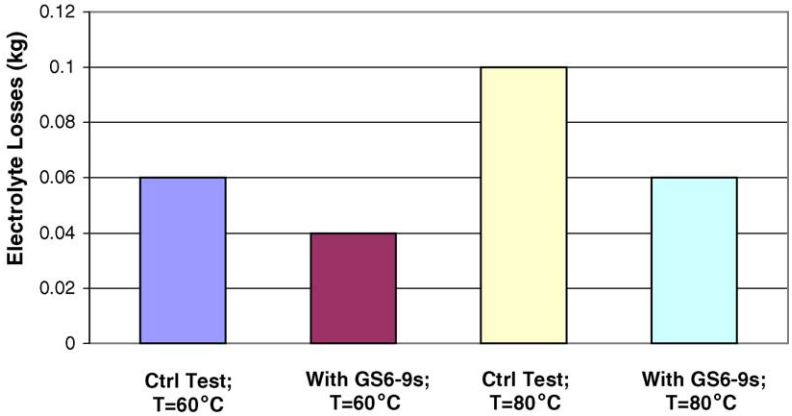

Fig. 8. Total electrolyte losses during a membrane-assisted lead-acid battery charging test with heat supply.

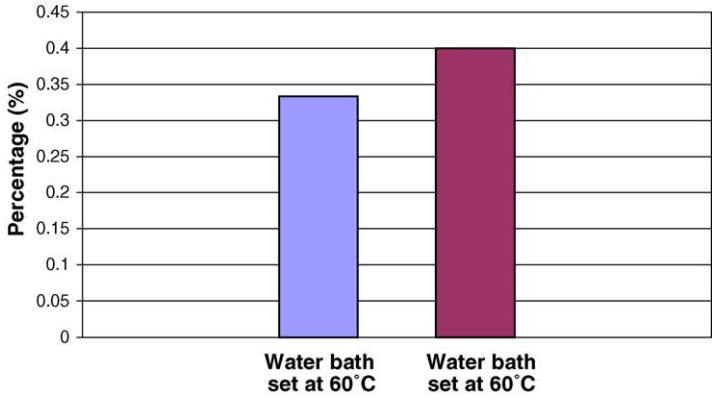

Fig. 9. Magnitude of electrolyte loss compared to the conventional lead-acid battery.

average, the rate of electrolyte loss for a conventional battery when the temperature is 80 °C is 33.33 g h^{-1}, while for the membrane-applied battery it is only 20 g h^{-1}.

As shown in Fig. 9 and by calculating using Eq (3.1) during the lead-acid battery charging process in the engine compartment, when the temperature reaches 60 °C, the membrane-assisted lead-acid battery can save up to 33.33% of electrolyte compared to the conventional battery. Meanwhile, when the temperature reaches 80 °C, the membrane-assisted lead-acid battery can save up to 40% of electrolyte during the charging process.

Comparing to the results from the previous charging test, the average electrolyte loss rate for the membrane-applied lead-acid battery at room temperature is 6.67 g h^{-1}, which is about 50% less than when the temperature is set at 60 °C, and 67% less than when the temperature is set at 80 °C. This means that high-temperature conditions have an enormous effect on the electyrolyte losses for a membrane-assisted lead-acid battery during charging. Although membrane application on a lead-acid battery can minimize up to 40% of electrolyte losses when the temperature is 80 °C, the losses can still be further minimized with preventive measures. This can

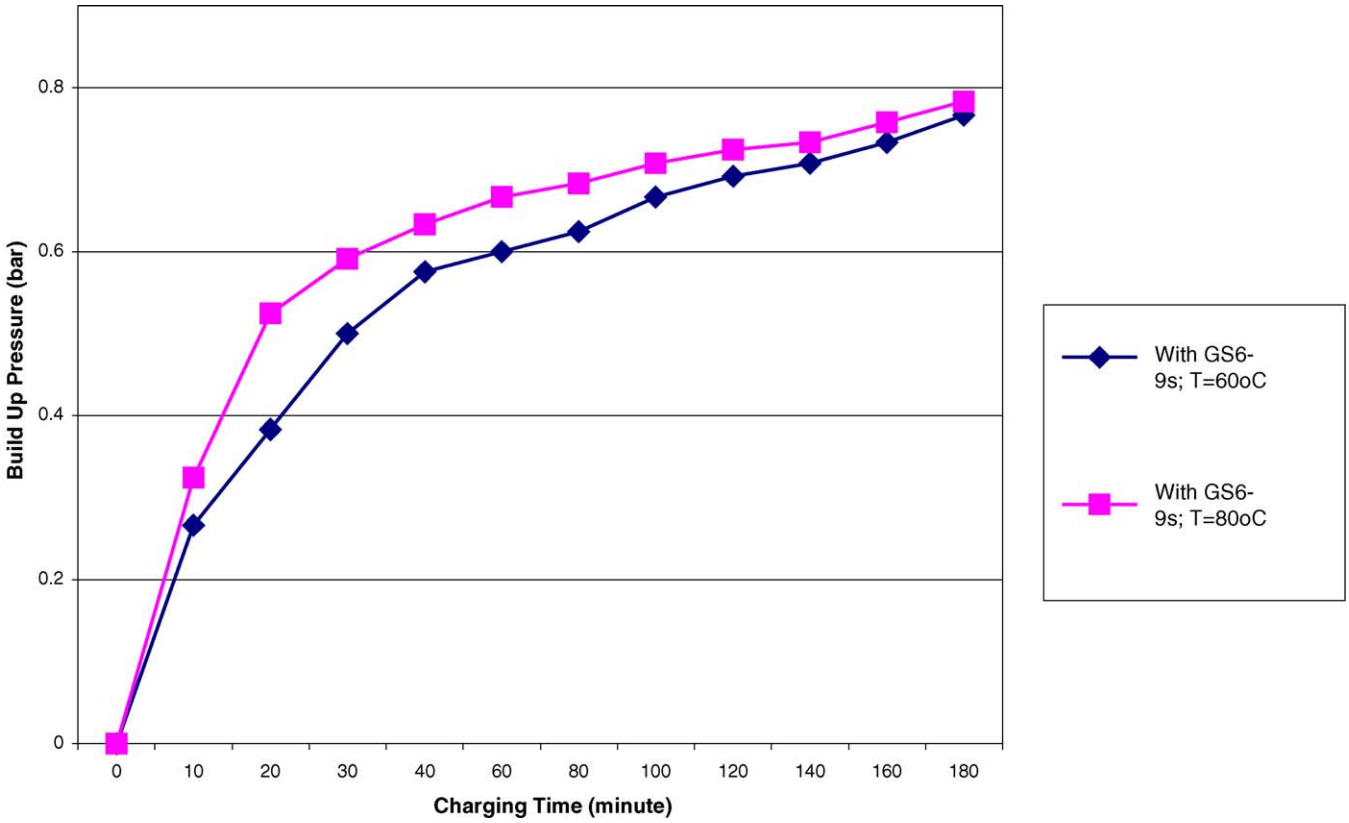

Fig. 10. Effect of water bath temperature on pressure build-up in a lead-acid battery during charging.

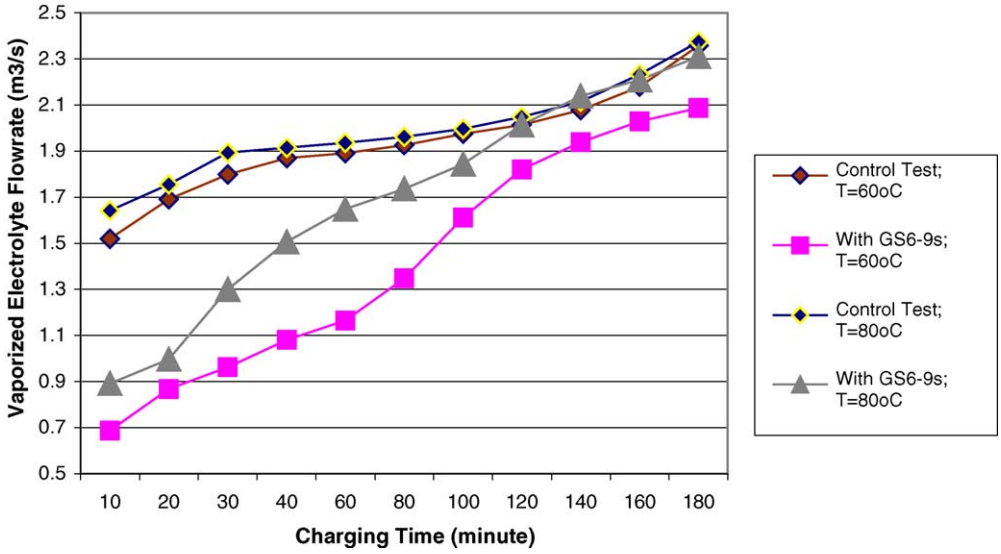

Fig. 11. Effect of water bath temperature on the flow rate profile of vaporized electrolyte.

be done with better heat insulation of the battery casing or altering the battery placement in the engine compartment, thus preventing heat being transferred into the battery.

The objective is to observe how the membrane performs in minimizing pressure build-up, even with the existence of an extreme temperature effect. Figs. 10 and 11 show the pressure build-up and vaporized electrolyte flow rate profiles during a membrane-applied lead-acid battery charging test with heat supply.

The pressure profile of the membrane-applied lead-acid battery charged in a water bath set at 60 and 80 °C showed almost similar increments of pressure for a battery that is charged without any heat supply. The only difference existing this time is that the final pressure is slightly higher than the previous test. When the temperature is set at 60 °C the final pressure is about 0.77 bar, while the final pressure with the temperature set at 80 °C is about 0.78 bar. This compares to the battery charged without any heat supply, where the final pressure was about 0.73 bar. This means that the effect of high temperature during charging is that the pressure build-up is increased by only a minimal amount. Therefore, in high-temperature conditions, the pressure build-up will not differ largely from the battery that is being charged at room temperature. This is due to the fact that the flow rate of vaporized electrolyte is consistently fast, even during the early stages of the charging process. With the smoothly permeating vaporized electrolyte, this condition has assisted the system to reduce the pressure build-up inside the battery.

From the vaporized electrolyte flow rate profile, it is seen that the vaporized electrolyte flow rates for both control tests run at 60 and 80 °C were very high. Compared to the membrane-applied lead-acid battery, the flow rate of vaporized electrolyte during the early stages of charging was quite low due to electrolyte-retaining characteristics of the membrane. As the charging progresses, the pressure increases and the vaporized electrolyte flow rate becomes faster in order to minimize the pressure build-up inside the battery.

4. Conclusion

The manipulation of polymer concentration and casting shear rate parameters during the preparation of gas-separation membranes has successfully produced the most suitable membrane featuring minimized electrolyte loss during the battery charging process. Based on the results obtained, the most suitable gas-separation membrane to be applied in the lead-acid batteries for the purpose of minimizing electrolyte loss is that prepared from the casting solution of 13% (w/w) PSF and 87% (w/w) DMF, and cast at the shear rate of 233 s^{-1}. Compared to the conventional battery, the application of this membrane into the lead-acid battery during the charging process can minimize of electrolyte loss by up to 75% at room temperature and by up to 40% at a temperature of 80 °C.

Temperature conditions during lead-acid battery charging has an important effect on electrolyte losses during the charging process. At a temperature of 60 °C, the electrolyte losses were double that of the batteries charged at room temperature. Meanwhile, at 80 °C, the electrolyte loss was three times that of the battery charged at room temperature.

The application of a gas-separation membrane in a lead-acid battery during the charging process has successfully functioned as an electrolyte-retaining device. The GS6 membrane can further be commercialized in membrane-assisted lead-acid battery with the introduction of a specially designed battery case top that features holders for the membranes to be affixed and which has been tightly sealed to eliminate traces of leakage. With the reasonably low membrane cost of about USD 0.4 per battery, the so-called membrane-assisted

lead-acid battery would often a remarkably good advantage over other lead-acid batteries offered in the market today, in terms of economic and technological perspective.

References

[1] H.R. Ibrahim, J. Power Sources 23 (1988) 47–51.
[2] J. Wong, J. Power Sources 40 (1992) 105–111.
[3] N. Hawkes, J. Power Sources 67 (1997) 213–218.
[4] P.S. da Silva, J. Power Sources 67 (1997) 3–6.
[5] G. Billard, J. Power Sources 38 (1992) 3–11.
[6] H.A. Kiehne, Battery Technology Handbook, 1st ed., Expert Verlag, Germany, 1989, pp. 1–27.
[7] D. Linden, Handbook of Batteries, 24, 3rd ed., McGraw-Hill, New York, 1995, 24.1–24.5.
[8] P. Ruetschi, J. Power Sources 127 (2004) 33–44.
[9] S. Bodoardo, M. Maja, N. Penazzi, J. Power Sources 55 (1995) 183–190.
[10] D. Berndt, J. Power Sources 100 (2001) 29–46.
[11] R.J. Ball, R. Evans, R. Stevens, J. Power Sources 104 (2002) 208–220.
[12] L. Torcheux, C. Rouvet, C.P. Vaurijoux, J. Power Sources 78 (1999) 147–155.
[13] R.H. Newnham, W.D.A. Baldsing, J. Power Sources 66 (1997) 27–39.
[14] J. Kwasnik, T. Pukacka, M. Paszkiewicz, B. Szczesniak, J. Power Sources 31 (1990) 135–138.
[15] F.E. Henn, C. Rouvet, A. de Guibert, P. Martue, J. Power Sources 63 (1996) 235–246.
[16] H. Dietz, S. Voss, H. Doring, J. Garche, K. Wiesener, J. Power Sources 31 (1990) 107–113.
[17] H. Dietz, L. Dittmar, D. Ohms, M. Radwan, K. Wiesener, J. Power Sources 40 (1992) 175–186.
[18] C. Armenta-Deu, J. Power Sources 70 (1998) 200–204.
[19] L.T. Lam, J.D. Douglas, R. Pillig, D.A.J. Rand, J. Power Sources 48 (1994) 219–232.
[20] M. Maja, N. Penazzi, J. Power Sources 22 (1988) 1–9.
[21] T.S. Chung, S.K. Teoh, X.D. Hu, J. Membr. Sci. 133 (1997) 161–175.
[22] H. Hachisuka, T. Ohara, K. Ikeda, J. Appl. Polym. Sci. 61 (1996) 1615–1619.
[23] A.F. Ismail, S.J. Shilton, I.R. Dunkin, S.L. Gallivan, J. Membr. Sci. 126 (1997) 133–137.
[24] S.J. Shilton, A.F. Ismail, I.R. Dunkin, S.L. Gallivan, P.J. Gough, Polymer 38 (1997) 2215–2220.
[25] S.J. Shilton, G. Bell, J. Ferguson, Polymer 37 (1994) 5327–5335.
[26] I.D. Sharpe, A.F. Ismail, S.J. Shilton, Separ. Purif. Technol. 17 (1999) 101–109.
[27] T.S. Chung, W.H. Lin, R.H. Vora, J. Membr. Sci. 167 (2000) 55–66.